Cohen and J. Lyle, *ibid.* **14**, 434 (1986); M. E. Varnes and J. E. Biaglow, *Cancer Res.* **39**, 2960 (1979). Nonprotein and total sulfhydryl content was determined by a modification of the Ellman method [G. L. Ellman, *Arch. Biochem. Biophys.* **82**, 70 (1959); J. Sedlak and R. H. Lindsay, *Anal. Biochem.* **25**, 192 (1968); T. W. Wong and G. F. Whitmore, *Radiat. Res.* **71**, 132 (1977); M. E. Varnes and J. E. Biaglow, above]. Cells (10^7) from the EMT-6 parent tumor line and each of the resistant lines were lysed in 6 ml of 0.02*M* EDTA. For nonprotein sulfhydryl determination, 5 ml of the cell lysate was treated with an equal volume of 10% trichloroacetic acid, then centrifuged at 500*g* for 5 min at 5°C. Four milliliters of the supernatant was adjusted to *p*H 8.9 with 0.2*M* tris buffer. Ellman's reagent [0.01*M* 5,5′-dithiobis(2-nitrobenzoic acid)] in methanol (Aldrich) (12.5 μl of sample per milliliter) was added, and color was allowed to develop for 30 min at room temperature. Total sulfhydryl content was determined by adding cell lysate (0.5 ml) to 0.02*M* tris buffer (1.5 ml, *p*H 8.2), followed by 0.1 ml of 0.01*M* 5,5′-dithiobis(2-nitrobenzoic acid) in methanol. After bringing the sample volume to 3 ml with methanol, the color was allowed to develop for 30 min at room temperature. All of the samples were filtered (0.45 μ*M*), and absorbance was read at 412 nm. Protein sulfhydryl content was determined from the difference between the total sulfhydryl content and nonprotein sulfhydryl content. Each measurement was repeated at least three times.

11. Animals were killed by cervical dislocation, and tumors were quickly excised for fixation in phosphate-buffered formalin (light microscopy) or Kamovsky's fixative (electron microscopy). After tissue processing by routine methods, sections were examined in a random fashion.
12. Tumor volume measurements began on day 7 after implantation of 2×10^6 tumor cells subcutaneously in the legs of BALB/c mice 8 to 10 weeks of age. We made three measurements (length, width, and depth) on each tumor using calipers and calculated the tumor volume assuming the tumor to be a hemiellipsoid. Data from the tumor volume measurements were analyzed with a computer program written for an Apple microcomputer. The program first derives the best-fit curve for each individual set of tumor volume data, then calculates the median, mean, and SEM for each experimental group. Measurements were made on nine individual tumors of each type.
13. BALB/c mice bearing EMT-6 parental tumors or EMT-6/CDDP tumors and non–tumor bearing animals were injected ip with CDDP at 10 mg/kg. Animals were killed at 11 time points after drug administration. Known wet weights of tumor, liver, kidney, skin, skeletal muscle, and blood were dissolved in a tissue solubilizer (Protosol; DuPont Biotechnology Systems), then analyzed by flameless atomic absorption spectroscopy. Platinum from a 15-μl sample injection volume was atomized from the walls of pyrolytically coated graphite tubes. A Perkin-Elmer Model 2380 atomic absorption spectrophotometer was used in conjunction with a Perkin-Elmer Model 400 graphite furnace to measure the absolute mass of platinum in the cell samples. Each measurement was made in triplicate in three independent experiments. [O. H. Drummer, A. Proudfoot, L. Howes, W. J. Louis, *Clin. Chim. Acta.* **136**, 65 (1984); T. S. Herman *et al.*, *Cancer Res.* **48**, 5101 (1988); T. S. Herman *et al.*, *ibid.*, p. 2335.]
14. The data were fitted to a triexponential equation of the form $C = A_0 e^{-kat} + B_0 e^{-\alpha t} + C_0 e^{-\beta t}$, which allowed derivation of the half times ($t_{1/2}$ for absorption, distribution, and elimination of the drug as well as calculation of the area under the curve of concentration versus time [R. L. Furner, R. K. Brown, G. Duncan, *Cancer Treat Rep.* **61**, 1637 (1977); R. K. Brown, G. Duncan, D. L. Hill, *ibid.* **64**, 643 (1980)].
15. BALB/c mice bearing EMT-6 parental tumors or EMT-6/CTX and non–tumor bearing animals were injected ip with 6 μCi of [*ring*-4-^{14}C]CTX (150 mg/kg; 52.5 mCi/mmol). The animals were killed at 11 time points after drug administration. Known wet weights of tumor, liver, kidney, skin, skeletal muscle, and blood were dissolved in a tissue solubilizer (Protosol; DuPont Biotechnology Systems), then counted by liquid scintillation in Aquasol (DuPont Biotechnology Systems).
16. W. D. Odell, *Adv. Intern. Med.* **34**, 325 (1989); S. E. Bates, *Semin. Oncol.* **14** (2), 102 (1987); B. Fisher *et al.*, *Cancer Res.* **49**, 1996 (1989).
17. CDDP and carboplatin pure powders were a gift from M. Abrams and D. Picker, Johnson-Matthey, Malvern, PA; 4-hydroperoxycyclophosphamide, used in vitro as an activated form of cyclophosphamide (Sigma), was a gift from O. M. Colvin; thiotepa was a gift from Lederle Laboratories, Pearl River, NY. Supported by National Cancer Institute grant P01-CA38497 and a grant from Bristol-Myers Co., Wallingford, CT.

20 November 1989; accepted 25 January 1990

Engineering Human Prolactin to Bind to the Human Growth Hormone Receptor

BRIAN C. CUNNINGHAM, DENNIS J. HENNER, JAMES A. WELLS*

A strategy of iterative site-directed mutagenesis and binding analysis was used to incorporate the receptor-binding determinants from human growth hormone (hGH) into the nonbinding homolog, human prolactin (hPRL). The complementary DNA for hPRL was cloned, expressed in *Escherichia coli*, and mutated to introduce sequentially those substitutions from hGH that were predicted by alanine-scanning mutagenesis and other studies to be most critical for binding to the hGH receptor from human liver. After seven rounds of site-specific mutagenesis, a variant of hPRL was obtained containing eight mutations with an association constant for the hGH receptor that was increased more than 10,000-fold. This hPRL variant binds one-sixth as strongly as wild-type hGH, but shares only 26 percent overall sequence identity with hGH. These studies show the feasibility of recruiting receptor-binding properties from distantly related and functionally divergent hormones and show that a detailed functional database can be used to guide the design of a protein-protein interface in the absence of direct structural information.

THE RECRUITMENT OF FUNCTIONAL properties within a family of homologous proteins by site-directed mutagenesis is a powerful approach for identifying determinants that modulate protein function. This is a useful design strategy because it makes it possible to combine into one homolog the most desirable functional characteristics (such as specificity, catalysis, stability, and immunogenicity) that are contained in the family. Previous recruitment studies (*1–4*) have relied on high-resolution structural data to target specific contact residues or entire units of secondary structure in order to exchange binding (*1, 2*) or enzymatic functions (*3, 4*) between homologs. We now show that the identification of receptor-binding determinants in hGH by high-resolution mutagenic analysis can be used in place of a structural model of the hormone-receptor complex to engineer hPRL, a distantly related and nonbinding homolog, so that it will bind to the hGH receptor.

Prolactin is a member of a family of homologous hormones that includes growth hormones, placental lactogens, and proliferins (*5*). Collectively, this group of hormones regulates a vast array of physiological effects important in growth, differentiation, and electrolyte balance, for example (*6*). These pharmacological effects are initiated by the binding of the hormones to specific cellular receptors. For example, hGH binds to both the lactogenic and somatogenic receptors and stimulates both lactation and bone growth. In contrast, hPRL binds only to the lactogenic receptor and stimulates lactation but not bone growth. The molecular basis for these differences in receptor-binding specificity is not understood.

Scanning mutagenesis methods (*7, 8*) have identified residues in hGH that strongly modulate binding to the extracellular fragment of the hGH receptor (also called the hGH-binding protein). The hGH-binding protein is more convenient and accurate for the assay of binding affinity because it can be expressed and purified to homogeneity in large amounts from *Escherichia coli* (*9*) and it retains binding specificity virtually identical to that of the full-length somatogenic receptor (*9, 10*). The amino acid side chains that modulate binding to the hGH-binding protein are located in three discontinuous segments of hGH. Together, these residues form a patch when mapped onto a crude

B. C. Cunningham and J. A. Wells, Department of Protein Engineering, Genentech, Inc., 460 Point San Bruno Boulevard, South San Francisco, CA 94080.
D. J. Henner, Department of Cell Genetics, Genentech, Inc., 460 Point San Bruno Boulevard, South San Francisco, CA 94080.

*To whom correspondence should be addressed.

structural model of hGH (Fig. 1) derived from a 2.8 Å folding diagram of porcine growth hormone (*11*).

Overall, hPRL shares only 23% sequence identity with hGH; in the three regions of hGH that are responsible for receptor binding, hPRL is 34% identical (not including insertions or deletions) (Fig. 2). By tailoring two of these analogous regions of hPRL to be like hGH, we have engineered a variant of hPRL containing eight mutations that binds tightly to the hGH receptor.

In order to identify which of the divergent residues in hPRL (Fig. 2) were most disruptive for binding to the hGH-binding protein, we introduced some of the hPRL residues into hGH (Table 1). Whereas single alanine substitutions in hGH at positions 58, 64, and 176 or asparagine substituted at position 178 strongly disrupts receptor binding (*8*), substitutions of hPRL residues into hGH at these positions have a lesser effect (Table 1). The conservative F176Y mutation (*12*) in hGH, which results in the incorporation of a larger residue, causes an eightfold reduction in affinity for the hGH-binding protein. The R64K substitution, which results in the incorporation of a smaller residue, shows slightly enhanced binding affinity. The largest disruptions caused by hPRL substitutions are at positions 176 and 178, suggesting that residues in the helix-4 region of hPRL strongly perturb the binding of hPRL to the hGH-binding protein.

The cDNA for hPRL was cloned from a human pituitary cDNA library (*13, 14*) and expressed intracellularly in *E. coli* (*15, 16*) with the use of the plasmid pBO760 (Fig. 3). The purified recombinant hPRL, refolded from inclusion bodies (*17*), retained a circular dichroism (CD) spectrum (Fig. 4) identical to natural hPRL (*18*). Other studies (*19*) showed the *E. coli*–derived hPRL to be equipotent in an hPRL enzyme-linked immunosorbent assay (ELISA) and an Nb2 cell bioassay (*20*). The recombinant hPRL, like intracellularly expressed hGH (*21*), retains its initiator methionine, but the extra residue has no apparent effect on the structure or function of either hormone.

Table 1. Dissociation constants (K_d) for the binding of hGH mutants (constructed by substituting alanine residues or residues from hPRL) to the extracellular domain of the hGH receptor. Mutants of hGH were prepared as described (*23*). The values of K_d for each analog were determined by competitive displacement of ^{125}I-labeled hGH bound to the purified recombinant hGH receptor as previously described (*7–10*). Variants are named as described (*12*). Values for the alanine mutants and R178N were taken from (*8*). WT, wild type; mut, mutant.

hGH mutant	K_d (n*M*) (mean ± SD)	K_d mut / K_d WT
WT	0.34 ± 0.04	1
158L	0.58 ± 0.11	1.7
158A	5.6 ± 1.4	16
R64K	0.2 ± 0.05	0.6
R64A	7.1 ± 1.6	21
F176Y	2.9 ± 0.5	8.6
F176A	5.4 ± 1.3	16
R178K	1.7 ± 0.3	5.1
R178N	2.9 ± 0.4	8.5

The affinity of hPRL for the hGH-binding protein is more than 10^5-fold lower than that of hGH (Table 2) and is below the detection limit of our binding assay. Initially, a combination of three divergent residues in helix 4 from hGH (H171D, N175T, and Y176F) were introduced into hPRL, which either alanine-scanning mutagenesis (*8*) or hPRL substitutions (Table 1) showed to be important for binding of hGH to the hGH-binding protein (Figs. 1 and 2). This triple mutant of hPRL exhibits detectable binding to the hGH-binding protein, albeit 14,000-fold weaker than that of hGH. Substitution of another important helix-4 residue (K178R) to produce a tetramutant (variant B, Table 2) strengthens binding more than 20 times to a level only 660-fold below that of wild-type hGH. Replacing the rest of helix 4 by substitution of hGH residues 184 to 188 into hPRL variant B does not enhance binding to the hGH-binding protein. However, the affinity of hPRL variant B is increased 3.5-fold by including E174A (variant C, Table 2), as is found when E174A is incorporated into hGH (*8*).

Having optimized binding affinity in the helix-4 region, we next concentrated on the loop region containing residues 54 to 74. Complete replacement of the loop region in hPRL with the sequence from hGH [hGH (54–74), Table 2] results in barely detectable binding to the hGH-binding protein. When this mutant is combined with variant

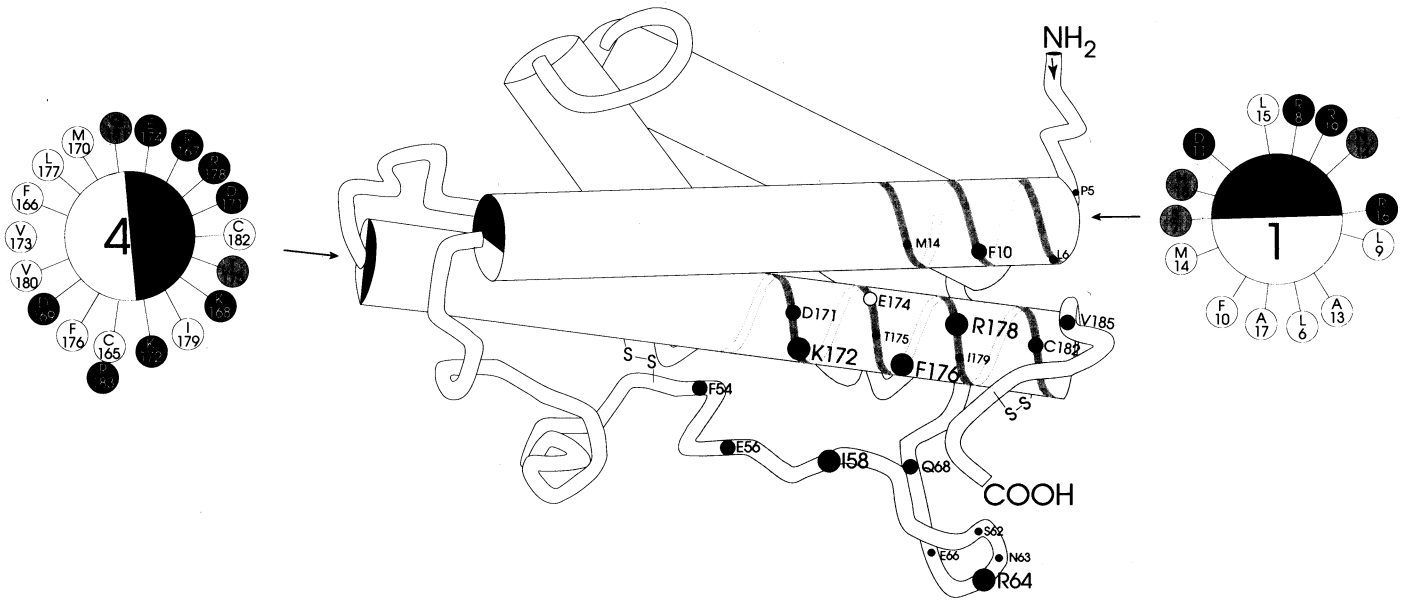

Fig. 1. Location of residues in hGH that strongly modulate its binding to the hGH-binding protein (shaded circle). Alanine substitutions (serine or asparagine in the case of T175 or R178, respectively) that cause a greater than tenfold reduction (●), a four- to tenfold reduction (•) or increase (○), or a two- to fourfold reduction (•) in binding affinity are indicated (*8*). Helical wheel projections in regions of α helix reveal their amphipathic quality (blackened, shaded, or nonshaded residues are charged, polar, or nonpolar, respectively). In helix-4 the most important determinants are on its hydrophilic face (shaded). The structural model (*7*) is derived from a folding diagram of porcine growth hormone determined crystallographically (*11*).

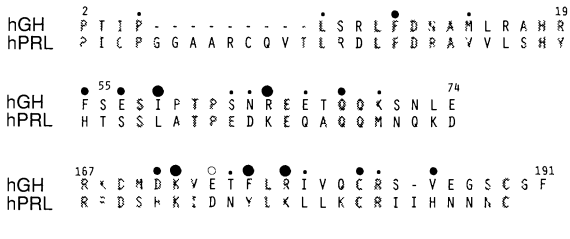

Fig. 2. Sequence comparison of hGH and hPRL in regions defined by homolog- (*7*) and alanine-scanning mutagenesis (*8*) to be important for binding. Identical residues are shaded and the numbering is based on the hGH sequence. The dashed lines show the positions of residues inserted into hPRL. Circles above the residues indicate sites at which mutations (described in Fig. 1) cause a greater than tenfold reduction (●), a four- to tenfold reduction (•) or increase (○), or a two- to fourfold reduction (•) in binding affinity. See (*12*) for single-letter amino acid code.

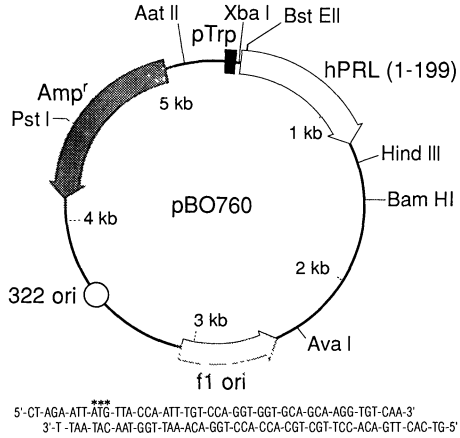

Fig. 3. Plasmid diagram of pBO760 used for intracellular expression of hPRL in *E. coli*. The *E. coli trp* promoter (indicated pTrp) derived from pHGH207-1 (*16*) directs transcription of the hPRL gene. The hPRL coding sequence [indicated as hPRL (1–199)] consisted of a 47-bp Xba I–Bst EII synthetic DNA cassette and the 720-bp Bst EII–Hind III fragment derived from the hPRL cDNA (*13, 14*). The sequence of the synthetic DNA cassette is shown below the plasmid diagram, where the initiation codon is indicated by asterisks. The phage f1 origin, pBR322 replication origin, and the pBR322 β-lactamase gene (Amp^r) were derived from pBO475 (*7*).

B, the affinity increases substantially. However, this new variant [B plus hGH (54–74), Table 2] is reduced in affinity to almost one-tenth that of variant B alone. Thus, it appears that some of the hGH residues in the 54 to 74 loop are not compatible with the hGH substitutions in helix 4 of hPRL.

To solve this problem, we selected from the 54 to 74 loop of hGH only those residues (seven in total) that greatly influence binding of hGH as shown by alanine-scanning mutagenesis (*8*). Although the R64A mutation in hGH causes a greater than 20-fold reduction in affinity, the R64K variant of hGH (which is an hPRL substitution) (Fig. 2) slightly enhances binding to the hGH-binding protein (Table 1). We therefore kept Lys^{64} in hPRL and incorporated only six of the seven substitutions from hGH into hPRL that were most disruptive when changed to alanine in hGH. This new mutant (B plus H54F:S56E:L58I:E62S:D63N:Q66E, Table 2) binds to the hGH-binding protein 50 times as strongly as B plus hGH (54–74) and has an affinity only 110 times less than that of wild-type hGH. However, the increase in affinity represents only a modest improvement (sixfold) over variant B alone and is less than we expected for strongly favorable interactions previously observed in the loop region for hGH (*8*). Therefore, we split the six mutations in the loop and combined three (H54F:S56E:L58I) with hPRL variant B. This heptamutant binds one-third as strongly as variant B alone; individually the three additional residues cause small disruptions in affinity when added to another hPRL mutant (see below). Therefore, we presumed that the three remaining mutations in the loop region (E62S:D63N:Q66E) enhanced affinity and so incorporated them into variant C (to give variant D). Indeed, this octamutant of hPRL has an affinity that is one-sixth that of hGH. Additional single mutations (H54F, S56E, L58I, A59P, N71S, and L179I) either reduce or have little effect on the affinity of hPRL variant D to the hGH-binding protein (Table 2). The total binding free energy of variant D is only about 1 kcal/mol less than that of wild-type hGH (12 versus 13 kcal/mol, respectively). It may be possible to improve further the binding affinity of hPRL variant D by including some other residues such as V14M or H185V, where alanine substitutions in hGH cause two- to fivefold reductions in binding affinity (Fig. 2).

The conformation of variant D is virtually indistinguishable from native hPRL by ELISA reactivity (*22*) or by CD spectral analysis (Fig. 4). The short-wave ultraviolet CD spectra (Fig. 4A) of hPRL or variant D are similar to hGH, suggesting a similar helical content; however, important differences from hGH in ellipticity at 208 and 224 nm are present as expected for hPRL (*18*). The long-wave ultraviolet CD spectra are virtually identical between wild-type hPRL and variant D (Fig. 4B), whereas the spectra of hGH and hPRL differ markedly because of variation between the two hormones in the number and microenvironment of aromatic residues. Thus, variant D has the ability to bind the hGH receptor while retaining a structural scaffold more like hPRL than hGH.

Our strategy for the design of the interface between the hGH receptor and the nonbinding homolog (hPRL) depended on a high-resolution functional database derived from the binding-competent homolog (hGH). Alanine-scanning mutagenesis of hGH (*8*) combined with analysis of the disruptive effects of hPRL substitutions in hGH (Table 1) directed us to introduce the cluster of divergent residues in helix 4 to

Table 2. Engineering residues in hPRL in order to permit binding to the hGH-binding protein. Mutants of hPRL were produced as described for hGH (*23*). Mutants were expressed (*15*), purified (*17*), and analyzed as described in Table 1. Multiple mutants are indicated by a series of single mutants (*12*) separated by colons. Codon numbering is based on the hGH sequence (Fig. 2). Mutants of hPRL designated hGH (184–188) and hGH (54–74) contain a complete replacement of hPRL residues with hGH residues from positions 184 to 188 and positions 54 to 74, respectively (Fig. 2).

hPRL mutant	K_d (nM) (mean ± SD)	K_d mutant / K_d hGH
hGH (wild type)	0.34 ± 0.04	1
hPRL (wild type)	>40,000	>100,000
A = H171D:N175T:Y176F	4,900 ± 1,400	14,000
B = A + K178R	220 ± 31	660
B + hGH (184–188)	260 ± 56	740
hGH (54–74)	~25,000 ± 14,000	~66,000
B + hGH (54–74)	2,000 ± 1,300	5,800
B + H54F:S56E:L58I:E62S:D63N:Q66E	36 ± 7	110
B + H54F:S56E:L58I	670 ± 80	2,000
C = (B + E174A)	68 ± 12	200
D = (C + E62S:D63N:Q66E	2.1 ± 0.3	6.2
D + H54F	4.4 ± 0.6	13
D + S56E	2.5 ± 0.3	7.4
D + L58I	3.6 ± 0.1	11
D + A59P	2.5 ± 0.7	7.4
D + N71S	3.6 ± 0.7	11
D + L179I	2.1 ± 0.4	6.2

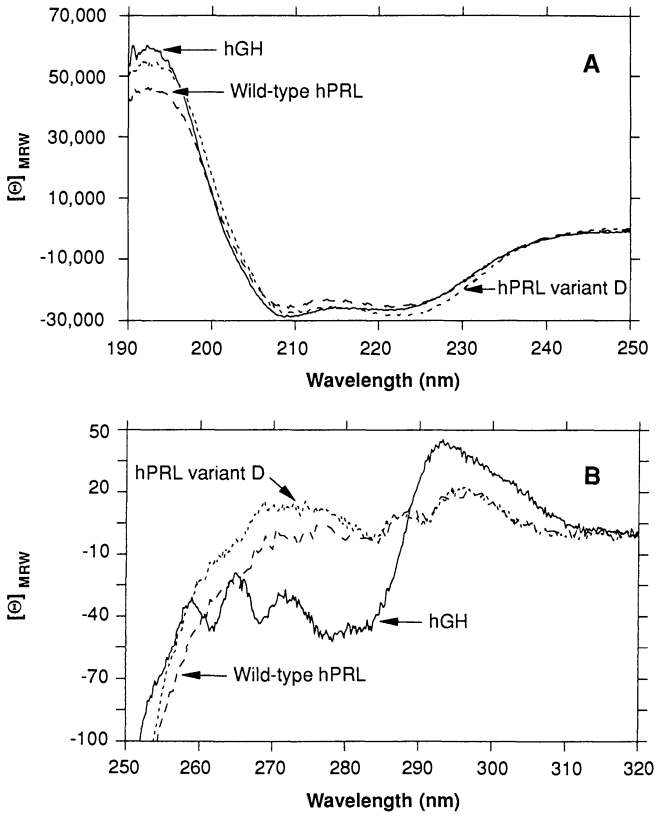

Fig. 4. CD spectra in the short-wave ultraviolet (**A**) or long-wave ultraviolet (**B**) of hGH (----), wild-type hPRL (– –), and hPRL variant D (- - - -) (Table 2). Spectra were collected on an Aviv Cary 60 spectropolarimeter. Ellipticity (θ) is expressed as mean residue weight (MRW).

initially achieve some binding affinity for hPRL. This was crucial because we were unable to detect any binding to the hGH-binding protein with wild-type hPRL, and it was necessary to introduce several hGH substitutions simultaneously into hPRL in order to bring the affinity within the detection range of our assay [dissociation constant (K_d) ≤50 μ*M*].

A number of iterative cycles of mutagenesis were necessary to converge on a combination of residues that permitted tight binding of hPRL to the hGH-binding protein. This approach relied on the assumption that the effect of the mutations on the free energy of binding would be somewhat additive, as was observed. For example, the E174A mutation enhanced the binding three- to fivefold when added to either hPRL variant C or hGH. Furthermore, to separate the mutations that were important for binding from those disruptive to binding in the 54 to 74 loop, we had to assemble this segment in stages. The cumulative nature of the mutational effects allows one to converge on the binding property in much the same way as proteins evolve, by cycles of natural variation and selection.

Previous protein engineering experiments have shown it is possible with high-resolution structural data to design binding properties by site-directed mutagenesis of contact residues (*3, 4*) or by replacement of entire units of secondary structure that participate in binding (*1, 2*). Here, the residues chosen to substitute were based on high-resolution functional, rather than structural, data. Moreover, to recruit the hGH receptor–binding properties into hPRL required selective residue replacements as opposed to substituting whole segments. For example, our data suggest that some of the residues in the 54 to 74 loop are crucial for the overall structure and should be left in place.

That the binding specificity for the hGH receptor could be incorporated into hPRL confirms the functional importance of particular residues for somatogenic receptor–binding, and provides compelling evidence for structural relatedness between hGH and hPRL despite their low sequence identity (23%). This provides a rational approach to access receptor-binding functions contained within this hormone family starting with either a growth hormone, prolactin, proliferin, or placental lactogen scaffold. Such hybrid hormones may have more useful properties as receptor agonists or antagonists and could be important for separating receptor-binding and activation as well as the pharmacological importance of receptor subtypes.

REFERENCES AND NOTES

1. R. P. Wharton and M. Ptashne, *Nature* **316**, 601 (1985).
2. P. T. Jones, P. H. Dear, J. Foote, M. S. Neuberger, G. Winter, *ibid.* **321**, 522 (1986).
3. J. A. Wells, B. C. Cunningham, T. P. Graycar, D. A. Estell, *Proc. Natl. Acad. Sci. U.S.A.* **84**, 5167 (1987).
4. H. M. Wilks *et al.*, *Science* **242**, 1541 (1988).
5. C. S. Nicoll, G. L. Mayer, S. M. Russell, *Endocrinol. Rev.* **7**, 169 (1986).
6. R. K. Chawla, J. S. Parks, D. Rudman, *Annu. Rev. Med.* **34**, 519 (1983); O. Isaksson, S. Eclen, J. O. Jansson, *Annu. Rev. Physiol.* **47**, 483 (1985).
7. B. C. Cunningham, P. Jhurani, P. Ng, J. A. Wells, *Science* **243**, 1330 (1989).
8. B. C. Cunningham and J. A. Wells, *ibid.* **244**, 1081 (1989). Reevaluation of the binding constant for the Thr175Ser mutation in hGH to the hGH-binding protein gives a K_d of 1.2 (± 0.3) n*M* not 5.9 (± 1.5) n*M* as previously reported.
9. G. Fuh *et al.*, *J. Biol. Chem.* **265**, 3111 (1990).
10. D. W. Leung *et al.*, *Nature* **330**, 537 (1987); S. A. Spencer *et al.*, *J. Biol. Chem.* **263**, 7862 (1988).
11. S. S. Abdel-Meguid *et al.*, *Proc. Natl. Acad. Sci. U.S.A.* **84**, 6434 (1987).
12. Variants are designated by the wild-type residue in single-letter abbreviation followed by its codon position (based on hGH numbering) and then the mutant residue. For example, I58L indicates a mutant in which isoleucine-58 is replaced by leucine. Abbreviations for the amino acid residues are: A, Ala; C, Cys; D, Asp; E, Glu; F, Phe; G, Gly; H, His; I, Ile; K, Lys; L, Leu; M, Met; N, Asn; P, Pro; Q, Gln; R, Arg; S, Ser; T, Thr; V, Val; W, Trp; and Y, Tyr.
13. The cDNA for hPRL was cloned from a human pituitary cDNA library in λgt10 [T. V Huynh, R. R. Young, R. W. Davis, in *DNA Cloning Techniques: A Practical Approach*, D. M. Glover, Ed. (IRL, Oxford, 1985), vol. 1, pp. 49–59] by hybridization [T. Maniatis, E. F. Fritsch, J. Sambrook, *Molecular Cloning: A Laboratory Manual* (Cold Spring Harbor Laboratory, Cold Spring Harbor, NY, 1982)] with oligonucleotide probes (25 nucleotides long) corresponding to the 5′ and 3′ ends of the cDNA sequence of hPRL (*14*). A near full-length cDNA clone was identified, and the 720-bp Bst II–Hind III fragment, extending from codon 12 to 55 bp past the stop codon, was subcloned into pUC118. The sequence was determined by the dideoxy method [F. Sanger, S. Nicklen, A. R. Coulson, *Proc. Natl. Acad. Sci. U.S.A.* **74**, 5463 (1977)] and matched exactly that previously reported (*14*).
14. N. E. Cooke, D. Coit, J. Shine, J. D. Baxter, J. A. Martial, *J. Biol. Chem.* **256**, 4007 (1981).
15. *Escherichia coli* cells (MM 294) containing pBO760 were grown at 37°C for 4 hours (or until the absorbance at 550 nm of the culture was 0.1 to 0.3) in 0.5-liter shake flasks containing 100 ml of M9 hycase medium [J. H. Miller, *Experiments in Molecular Genetics* (Cold Spring Harbor Laboratory, Cold Spring Harbor, NY, 1972)] containing carbenicillin (15 μg/ml). For larger batches, the culture was scaled up in a 10-liter fermentor. Indole acrylic acid was added (final concentration, 50 μg/ml) to induce the *trp* promoter (*16*). Cells were grown an additional 6 to 8 hours and then harvested by centrifugation. Cell fractionation experiments showed that hPRL was located almost exclusively in inclusion bodies and represented 2 to 5% of the total cell protein as analyzed by SDS–polyacrylamide gel electrophoresis (SDS-PAGE) (B. C. Cunningham, D. J. Henner, J. A. Wells, unpublished data).
16. H. A. deBoer, L. J. Comstock, D. Yansura, H. Heyneker, in *Promoters: Structure and Function*, R. L. Rodriguez and M. J. Chamberlin, Eds. (Praeger, New York, 1982), pp. 462–481.
17. Inclusion particles containing hPRL were isolated from 50 g of wet cell paste as described [M. E. Winkler and M. Blaber, *Biochemistry* **25**, 4041 (1986)]. The hPRL was refolded by solubilizing the inclusion particles in 156 ml of 8*M* guanidinium hydrochloride in TE buffer [10 m*M* tris (*p*H 8.0) and 1 m*M* EDTA] containing 0.3 g of reduced glutathione (Sigma)[A. K. Ahmed, S. W. Schaffer, D. B. Wetlaufer, *J. Biol. Chem.* **250**, 8477 (1975)]. After gentle stirring at room temperature for 30 min, the mixture was chilled to 0°C and diluted with 844 ml of cold TE buffer containing 0.6 g of oxidized glutathione. The solution was stirred slowly overnight at 4°C and dialyzed against 4 liters of TE buffer, which was replaced three times over 24 hours. Insoluble material was removed by centrifugation (10,000*g* for 20 min). The refolded and solubilized hPRL was precipitated with 45% satu-

rated $(NH_4)_2SO_4$ and stirred 2.5 hours at room temperature. The precipitate was collected by centrifugation (12,000*g* for 30 min) and dissolved in 5 ml of TE buffer. After 30 min at room temperature, the solution was clarified by centrifugation (10,000*g* for 10 min) and filtered through a Millipore filter (0.45 μm). The solution was dialyzed against 0.5 liters of TE buffer overnight at 4°C. The hPRL (85% pure) was finally purified to homogeneity (>95%) by fast-performance liquid chromatography (FPLC) and DEAE fast-flow matrix essentially as described for the purification of hGH (*7*). After reduction, the purified hPRL shows a pronounced retardation in mobility by SDS-PAGE (as seen for hGH) suggesting that disulfide bonds have formed [S. Pollit and H. Zalkin, *J. Bacteriol.* **153**, 27 (1983)]. The concentrations of hPRL and hPRL mutants were determined by measuring absorbance at 280 nm and by using a calculated extinction coefficient of $\epsilon_{280}^{0.1\%} = 0.9$ [D. B. Wetlaufer, *Adv. Protein Chem.* **17**, 303 (1962)], which was adjusted accordingly when variants contained mutations in aromatic residues. Concentration values determined by absorbance agreed to within 10% of those determined by laser densitometry of proteins subjected to SDS-PAGE and stained with Coomassie blue for hGH (*7, 8*).

18. T. A. Bewley, *Recent Prog. Horm. Res.* **35**, 155 (1979).
19. B. C. Cunningham, P. Jardieu, J. A. Wells, unpublished data.
20. T. Tanaka *et al.*, *J. Clin. Endocrinol. Metab.* **51**, 1058 (1980).
21. K. C. Olson *et al.*, *Nature* **293**, 408 (1981).
22. B. C. Cunningham and J. A. Wells, unpublished data.
23. For site-specific mutagenesis [M. J. Zoller and M. Smith, *Nucleic Acids Res.* **10**, 6487 (1982)], a synthetic hGH gene template was used that contained multiple unique restriction sites (*7*). Enrichment for mutant clones was obtained with the use of a mismatch repair-deficient strain of *E. coli*, *mut L* [B. Kramer, W. Kramer, H. J. Fritz, *Cell* **38**, 879 (1984)] and by designing mutagenic oligonucleotides to either introduce or eliminate a nearby unique restriction site so that restriction-purification or restriction-selection [J. A. Wells, B. C. Cunningham, T. P. Graycar, D. A. Estell, *Philos. Trans. R. Soc. London Ser. A* **317**, 415 (1986)], respectively, could be applied to the first pool of plasmid DNA obtained after transformation of the in vitro–generated heteroduplex. All oligonucleotides were designed to have 12 and 10 bp of exact match at their 5′ and 3′ ends, respectively. Variants of hGH were secreted into the periplasmic space of *E. coli* [C. N. Chang, M. Rey, B. Bochner, H. Heynecker, G. Gray, *Gene* **55**, 189 (1987)] and purified as described (*7, 8*).
24. We thank J. Heinrich for technical assistance in cloning hPRL; E. Chen for sequencing the hPRL cDNA clone; M. Mulkerrin for providing CD spectra; P. Carter and T. Kossiakoff for helpful comments on the manuscript; P. Jardieu for Nb2 cell assays; G. Fuh for providing purified hGH-binding protein; P. Ng, P. Jhurani, and M. Vasser for synthetic oligonucleotides; and W. Henzel for NH_2-terminal protein sequencing.

30 November 1989; accepted 29 January 1990

Direct Gene Transfer into Mouse Muscle in Vivo

JON A. WOLFF,* ROBERT W. MALONE, PHILLIP WILLIAMS, WANG CHONG, GYULA ACSADI, AGNES JANI, PHILIP L. FELGNER

RNA and DNA expression vectors containing genes for chloramphenicol acetyltransferase, luciferase, and β-galactosidase were separately injected into mouse skeletal muscle in vivo. Protein expression was readily detected in all cases, and no special delivery system was required for these effects. The extent of expression from both the RNA and DNA constructs was comparable to that obtained from fibroblasts transfected in vitro under optimal conditions. In situ cytochemical staining for β-galactosidase activity was localized to muscle cells following injection of the β-galactosidase DNA vector. After injection of the DNA luciferase expression vector, luciferase activity was present in the muscle for at least 2 months.

MOST EFFORTS TOWARD POSTNATAL gene therapy have relied on indirect means of introducing new genetic information into tissues: target cells are removed from the body, infected with viral vectors carrying the new genetic information, and then reimplanted into the body (*1*). For some applications, direct introduction of genes into tissues in vivo, without the use of viral vectors, would be useful. Direct in vivo gene transfer into postnatal animals has been achieved with formulations of DNA encapsulated in liposomes, DNA entrapped in proteoliposomes containing viral envelope receptor proteins (*2*), calcium phosphate–coprecipitated DNA (*3*), and DNA coupled to a polylysine-glycoprotein carrier complex (*4*). In vivo infectivity of cloned viral DNA sequences after direct intrahepatic injection with or without formation of calcium phosphate coprecipitates has also been described (*5*). With the use of cationic lipid vesicles (*6*), mRNA sequences containing elements that enhance stability can be efficiently translated in tissue culture cells (*7*) and in *Xenopus laevis* embryos (*8*). We now show that injection of pure RNA or DNA directly into mouse skeletal muscle results in significant expression of reporter genes within the muscle cells.

The quadricep muscles of mice were injected (*9*) with either 100 μg of pRSVCAT DNA plasmid (*10*) or 100 μg of βgCATβ-gA_n RNA (*7, 11, 12*). The RNA consists of the chloramphenicol acetyl transferase (CAT) coding sequences flanked by β-globin 5′ and 3′ untranslated sequences and a 3′ polyadenylate tract. CAT activity was readily detected in all four RNA injection sites 18 hours after injection and in all six DNA injection sites 48 hours after injection (Fig. 1). Extracts from two of the four RNA injection sites (Fig. 1, lanes 6 and 8) and from two of the six DNA injection sites (Fig. 1, lanes 11 and 20) contained amounts of CAT activity comparable to those obtained from fibroblasts transiently transfected with the corresponding constructs in vitro under optimal conditions (Fig. 1, lanes 9 and 10 and 21 to 24, respectively). The average total amount of CAT activity expressed in muscle was 960 pg for the RNA injections and 116 pg for the DNA injections. The variability in CAT activity recovered from different muscle sites probably represents variability inherent in the injection and extraction technique, because significant variability was observed when pure CAT protein or pRSVCAT-transfected fibroblasts were injected into the muscle sites and immediately excised for measurement of CAT activity. CAT activity was also recovered from abdominal muscle injected with the RNA or DNA CAT vectors (*13*), indicating that other muscles can take up and express polynucleotides.

The site of gene expression was determined for the pRSV*lac-Z* DNA vector (*14*) expressing the *Escherichia coli* β-galactosidase gene (Fig. 2). Seven days after a single injection of 100 μg of pRSV*lac-Z* DNA into individual quadricep muscles, the entire muscles were removed, and every fifth 15-μm cross section was histochemically stained for β-galactosidase activity. Approximately 60 (1.5%) of the ~4000 muscle cells that comprise the entire quadriceps and ~10 to 30% of the cells within the injection area were stained blue (Fig. 2, A and B). Positive β-galactosidase staining within some individual muscle cells was at least 1.2 mm deep on serial cross sections (Fig. 2, D to F), which may be the result of either transfection into multiple nuclei or the ability of cytoplasmic proteins expressed from one nucleus to be distributed widely within the muscle cell (*15*). Longitudinal sectioning also revealed β-galactosidase staining within muscle cells for at least 400 μm (Fig. 2C). Fainter blue staining often appeared in the bordering areas of cells adjacent to intensely stained cells. This most likely represents an artifact of the histochemical β-galactosidase

J. A. Wolff, P. Williams, W. Chong, G. Acsadi, A. Jani, Departments of Pediatrics and Genetics, Waisman Center, University of Wisconsin, Madison, WI 53706.
R. W. Malone and P. L. Felgner, Vical Inc., San Diego, CA 92121.

*To whom correspondence should be addressed.